BEAM-BEAM INTERACTIONS IN p-p STORAGE RINGS

E. Keil

CERN
Geneva, Switzerland

1. Overview

There are two lectures: The first one (sections 2 to 5) deals with the theoretical aspects of the beam-beam interaction, and the second one (sections 6 to 8) describes the results of experiments in the ISR.

Section 3 describes the strength of the beam-beam interaction in terms of the linear tune shift ΔQ which has been calculated for several models. Because of the non-uniform density distribution in the beam the force results in a tune spread. This can be calculated by a perturbation method as explained in section 4. Section 5 discusses the simulation of the beam-beam interaction on a computer. Finally, section 6 reviews beam-beam phenomena observed in the CERN-ISR. These include the absence of observable beam-beam effects in unbunched beams, overlap knock-out resonances, collisions between a low-energy beam and a high-intensity stack, experiments with a nonlinear lens, and experiments with a high-β insertion. Section 7 contains a few concluding remarks.

2. Preliminaries

2.1 The Lorentz force due to a moving bunch

A moving bunch with charge Ne produces a current Ne v and hence generates both electric and magnetic fields yielding a Lorentz force $\vec{F}$ on a test particle moving with velocity v_1

$$\vec{F} = e\,\vec{E} + e\,\vec{v}_1 \times \vec{B} \tag{1}$$

The field may be obtained by a) observing that the bunch produces only an electric field in its rest frame and by b) using the transformation rules for electromagnetic fields

$$\begin{aligned} E_{\parallel} &= E_{\parallel}' & B_{\parallel} &= 0 \\ E_{\perp} &= \gamma_2\, E_{\perp}' & B_{\perp} &= -\frac{\gamma_2}{c^2}\,\vec{v}_2 \times \vec{E}' \end{aligned} \tag{2}$$

Here the primed quantities refer to the rest frame, v_2 is the velocity of the bunch and γ_2 the corresponding relativistic factor. Assuming that the bunch moves in the negative s-direction we obtain, by combining (1) and (2)

$$F_\perp = (1 + \beta_1\beta_2)\ e\ \gamma_2\ E_\perp' = (1 + \beta_1\beta_2)\ e\ E_\perp \tag{3}$$

Therefore, in order to obtain the Lorentz force, it is sufficient to find the solution for the electrostatic field and to multiply the result by $e(1 + \beta_1\beta_2)$. When the beam and the test particle travel in the same direction, the factor becomes $1 - \beta_1\beta_2$ and gives rise to the well-known cancellation of space charge effects as $1/\gamma^2$.

2.2 Beam-beam tune shift

The tune shift due to a gradient perturbation K(s) is given by

$$\Delta Q_x = \frac{1}{4\pi} \int \beta_x(s)\ K_x(s)\ ds \tag{4}$$

In a purely magnetic field $K_x(s)$ is defined as

$$K_x = \frac{1}{B\rho}\ \frac{\partial B_y}{\partial x} \tag{5}$$

Using the Lorentz force (3), K_x can be written as follows

$$K_x = \frac{(1 + \beta_1\beta_2)}{B\rho\ v_1}\ \frac{\partial E_x}{\partial x} = \frac{(1 + \beta_1\beta_2)e}{mc^2\ \beta_1^2\ \gamma_1}\ \frac{\partial E_x}{\partial x} \tag{6}$$

For the y direction, the calculation is analogous, and gives

$$K_y = \frac{(1 + \beta_1\beta_2)}{B\rho\ v_1}\ \frac{\partial E_y}{\partial y} = \frac{(1 + \beta_1\beta_2)e}{mc^2\ \beta_1^2\ \gamma_1}\ \frac{\partial E_y}{\partial y} \tag{7}$$

2.3 The electric field of a Gaussian bunch

Assuming a 3-dimensional Gaussian charge distribution in the bunch

$$\rho = \frac{Ne}{(2\pi)^{3/2}\ \sigma_x\sigma_y\sigma_s}\ \exp\left[-\frac{x^2}{2\sigma_x^2} - \frac{y^2}{2\sigma_y^2} - \frac{s^2}{2\sigma_s^2}\right] \tag{8}$$

the potential is given by [1)]

$$V = -\frac{Ne}{4\pi^{3/2}\,\varepsilon_0}\int_0^\infty \frac{1-\exp\left[-\frac{x^2}{2\sigma_x^2+t}-\frac{y^2}{2\sigma_y^2+t}-\frac{s^2}{2\sigma_s^2+t}\right]}{\left[(2\sigma_x^2+t)(2\sigma_y^2+t)(2\sigma_s^2+t)\right]^{1/2}}\,dt \tag{9}$$

For a charge distribution which is uniform in the s direction and Gaussian in the x and y direction we have

$$\rho = \frac{n\,e}{2\pi\,\sigma_x\sigma_y}\exp\left(-\frac{x^2}{2\sigma_x^2}-\frac{y^2}{2\sigma_y^2}\right) \tag{10}$$

and

$$V = -\frac{n\,e}{4\pi\,\varepsilon_0}\int_0^\infty \frac{1-\exp\left[-\frac{x^2}{2\sigma_x^2+t}-\frac{y^2}{2\sigma_y^2+t}\right]}{\left[(2\sigma_x^2+t)(2\sigma_y^2+t)\right]^{1/2}}\,dt \tag{11}$$

Here, n is the line (number) density of particles.

3. Linear Beam-Beam Tune Shift

3.1 Beam-beam tune shift due to a cylindrical uniform bunch

We now have all the elements needed for the evaluation of a simple example of the beam-beam tune shift: we take a cylindrical bunch of radius a and length ℓ, containing N particles in a uniform density distribution as shown in Fig. 1. This model is rather unrealistic but it gives the answers without the use of higher functions, tables of integrals, or computers. When the bunch collides with a test particle, the latter remains inside the bunch only for a distance $\ell/2$ as becomes clear when the motion of the bunch and the particle is followed in more detail, as shown in Fig. 2. If we assume that $\beta(s)$ and $K(s)$ are independent of s, (4) may be simplified and becomes

$$\Delta Q_z = \frac{\ell\,\beta_z\,K_z}{8\pi} \tag{12}$$

Here, z stands for either x or y.

In order to obtain K(s) from (6) or (7), we need $\partial E_z/\partial z$. Since the bunch length ℓ will usually be much larger than the bunch radius a, it is justified to calculate E_z in a two-dimensional model, i.e. by assuming $\ell \to \infty$ while the line density N/ℓ remains constant. Using Gauss' theorem for any vector $\vec{V}$

$$\oint \vec{V}\,d\sigma = \int \operatorname{div}\vec{V}\,d\tau \tag{13}$$

yields the following value for the electric field gradient

$$\frac{\partial E_z}{\partial z} = \frac{\rho}{2\varepsilon_0} \tag{14}$$

where ρ is the charge density

$$\rho = \frac{Ne}{\pi\, a^2\, \ell} \tag{15}$$

Putting everything together, we obtain

$$\Delta Q_z = \frac{(1 + \beta_1\beta_2)\, \beta_z\, r_0\, N}{4\pi\, a^2\, {\beta_1}^2\, \gamma_1} \tag{16}$$

Here, we have introduced the classical particle radius $r_0 = e^2/4\pi\, \varepsilon_0\, mc^2$. It should be noted that γ_2 and ℓ do not appear in (16).

3.2 Beam-beam tune shift due to head-on collisions with a Gaussian bunch

From (9) we obtain the following formula for $\partial E_x/\partial x$ at $x = y = 0$, and at a distance s' from the bunch centre in the longitudinal direction

$$\frac{\partial E_x}{\partial x} = \frac{Ne}{2\pi^{3/2}\, \varepsilon_0} \int_0^\infty \frac{\exp\left(-\dfrac{s'^2}{2\sigma_s^2 + t}\right) dt}{(2\sigma_x^2 + t)^{3/2}\, \left[(2\sigma_y^2 + t)(2\sigma_s^2 + t)\right]^{1/2}} \tag{17}$$

The integral can be simplified by noting that the main contribution comes from the interval where $t < 2\sigma_x^2$ or $2\sigma_y^2$. Since $\sigma_s >> \sigma_x, \sigma_y$ only a small error is introduced by removing the σ_s term from the integral.

$$\frac{\partial E_x}{\partial x} \approx \frac{Ne}{2\pi^{3/2}\, \varepsilon_0}\, \frac{\exp(-s'^2/2\sigma_s^2)}{\sigma_s \sqrt{2}} \int_0^\infty \frac{dt}{(2\sigma_x^2 + t)^{3/2}\, (2\sigma_y^2 + t)^{1/2}} \tag{18}$$

The integration yields

$$\frac{\partial E_x}{\partial x} \approx \frac{Ne}{2\pi^{3/2}\, 2^{1/2}\, \varepsilon_0}\, \frac{\exp(-s'^2/2\sigma_s^2)}{\sigma_s \sigma_x (\sigma_x + \sigma_y)} \tag{19}$$

We now have all the components required for the tune shift calculation. When using (19) in (4) we must evaluate the field at a distance s' given by

$$s' = 2s \tag{20}$$

as may be seen from Fig. 2. Thus

$$\Delta Q_x = \frac{1}{4\pi} \int \beta_x(s) \; \frac{(1 + \beta_1\beta_2)}{B \rho v_1} \; \frac{Ne}{2\pi^{3/2} 2^{1/2} \varepsilon_0} \; \frac{\exp(-2s^2/\sigma_s^2)ds}{\sigma_s\sigma_x(\sigma_x + \sigma_y)} \tag{21}$$

which becomes, for $\beta_z(s) = \text{const}$

$$\Delta Q_x = \frac{\beta_x}{4\pi} \; \frac{(1 + \beta_1\beta_2)}{B \rho v_1} \; \frac{Ne}{2\pi^{3/2} 2^{1/2} \varepsilon_0} \; \frac{\sigma_s}{\sigma_s 2^{1/2}} \; \frac{\pi^{1/2}}{\sigma_x(\sigma_x + \sigma_y)} \tag{22}$$

This expression can be simplified by rearranging terms, and by introducing the classical particle radius r_0

$$\Delta Q_x = \frac{\beta_x N r_0(1 + \beta_1\beta_2)}{4\pi \beta_1^2 \gamma_1 \sigma_x(\sigma_x + \sigma_y)} \tag{23}$$

The result for ΔQ_y is obtained by interchanging the indices x and y

$$\Delta Q_y = \frac{\beta_y N r_0(1 + \beta_1\beta_2)}{4\pi \beta_1^2 \gamma_1 \sigma_y(\sigma_x + \sigma_y)} \tag{24}$$

3.3 Validity of the simple formulae

When deriving (16), (23) and (24), β_x and β_y and the bunch dimensions σ_x, σ_y, σ_s were taken to be constant. In the vicinity of a minimum, β_x and β_y vary as follows

$$\beta_z = \beta_z^* + \frac{s^2}{\beta_z^*} \tag{25}$$

Most of the contributions to the integrals leading to (23) and (24) come from regions with $|s| \lesssim \sigma_s$. Replacing $\beta_z(s)$ by β_z^* without an appreciable error implies that $\sigma_s^2/\beta_z^* \ll \beta_z^*$ or $\sigma_s \ll \beta_z^*$. The beam sizes σ_x and σ_y vary in proportion to $\sqrt{\beta_z}$, and hence the assumption of a Gaussian bunch shape also breaks down when the β_z variation becomes too large. This also happens when the condition $\sigma_s \ll \beta_z^*$ is violated. Since these considerations play a central rôle in the beam-beam tune shift calculation for unbunched beams, we shall not enlarge on them now.

3.4 Unbunched uniform ribbon beam - large crossing angle

We assume that two beams with width w and height h cross horizontally at an angle ψ, as shown in Fig. 3. As long as $h \ll w$, we may assume that the electric

field has only an E_y component, which may be obtained by using Gauss' law

$$E_y = \frac{n\ e\ y}{\varepsilon_0\ w\ h} \tag{26}$$

The beam collide for a distance ℓ given by

$$\ell = w/\sin\psi \tag{27}$$

Combining (4), (6), (26) and (27) gives

$$\Delta Q_y = \frac{(1 + \beta_1\beta_2)\ \beta_y\ n\ r_0}{\sin\psi\ \beta_1^{\,2}\ \gamma_1\ h} \tag{28}$$

Again, the variations of β_y and w and h with the distance s have been neglected. Also, it has been assumed that the electromagnetic beam-beam interaction takes place only while the beams overlap.

3.5 Gaussian circular beam - small angle - low-β insertion

For future storage rings a different model is more appropriate since the beams cross at small angles in a low-β insertion. This situation has been analysed for beams with circular symmetry [2], and for beams with elliptic geometry [3]. The expressions for elliptic geometry will be given. The formulae for circular geometry are special cases of them.

Consider a vertical crossing at a small angle α in the co-ordinate system shown in Fig. 4. From the potential (11) we obtain for the field gradients a distance y' above the beam

$$\left.\frac{\partial E_x}{\partial x}\right|_{x=o} = \frac{n\ e}{4\pi\ \varepsilon_0\ \sigma_y^{\,2}}\ F_x(Y, K) \tag{29}$$

$$\left.\frac{\partial E_y}{\partial y}\right|_{x=o} = \frac{n\ e}{4\pi\ \varepsilon_0\ \sigma_y^{\,2}}\ F_y(Y, K) \tag{30}$$

where

$$F_x(Y, K) = \frac{2}{K^2 - 1}\left[1 - \frac{\exp(-Y^2)}{K} - \frac{\sqrt{\pi}\ Y}{\sqrt{K^2 - 1}}\ \phi(Y, K)\right] \tag{31}$$

$$F_y(Y, K) = -\frac{2}{K^2 - 1}\left[1 - K\exp(-Y^2) - \frac{\sqrt{\pi}\ Y}{\sqrt{K^2 - 1}}\ \phi(Y, K)\right] \tag{32}$$

where

$$\phi(Y, K) = \exp(-Y^2)\, w\left(\frac{i K Y}{\sqrt{K^2 - 1}}\right) - w\left(\frac{i Y}{\sqrt{K^2 - 1}}\right) \tag{33}$$

and

$$Y = \frac{y'}{\sigma_y \sqrt{2}} \qquad K = \sigma_x/\sigma_y \tag{34}$$

and w(z) is the complex error function, defined by

$$w(z) = \exp(-z^2)\left(1 + \frac{2i}{\sqrt{\pi}} \int_0^z \exp(t^2)dt\right) \tag{35}$$

For a test particle moving along the s axis, one has

$$y' = s\,\alpha \tag{36}$$

and hence the tune shifts become, by combining (4), (6) and (29) or (30)

$$\Delta Q_x = \frac{(1 + \beta_1\beta_2)}{4\pi\ \beta_1{}^2\ \gamma_1} \int \frac{\beta_x(s)\ r_0}{\sigma_y{}^2(s)}\ F_x\left(\frac{s\,\alpha}{\sigma_y(s)\ \sqrt{2}},\quad K(s)\right) ds \tag{37}$$

$$\Delta Q_x = \frac{(1 + \beta_1\beta_2)}{4\pi\ \beta_1{}^2\ \gamma_1} \int \frac{\beta_y(s)\ r_0}{\sigma_y{}^2(s)}\ F_y\left(\frac{s\,\alpha}{\sigma_y(s)\ \sqrt{2}},\quad K(s)\right) ds \tag{38}$$

Here it must be remembered that σ_x, σ_y, β_x and β_y are all functions of s or s'. The above integrals cannot be evaluated analytically for the general case. Results for some special cases can be found in the references.

When the crossing angle is large compared to the beam divergence, i.e. if $\eta = \beta_x{}^*\ \alpha/\sigma_x{}^* >> 1$, (37) tends towards the Gaussian beam equivalent of (28); for vertical crossing

$$\Delta Q_x = \left(\frac{2}{\pi}\right)^{\frac{1}{2}}\ \frac{n\ r_0\ \beta_x{}^*}{\gamma\ \sigma_x{}^*\ \alpha} \tag{39}$$

On the other hand, the tune shift is bigger than that given by (39) if $\eta \approx 1$. In this case the electromagnetic beam-beam interaction extends over a larger region than the physical overlapping of the two beams. The contribution of the region where the beams are close but not overlapping has been called long-range tune shift. This phenomenon can be avoided by choosing the crossing angle sufficiently large, at a small loss of luminosity.

4. Tune Spread in Beam-Beam Collisions

Since the force on the other beam is nonlinear for all realistic beam density distributions, the tune shift is a function of the betatron amplitudes of the test particle. This variation and the resulting distribution functions have been calculated for a circular beam [4] and an elliptic beam [5] with Gaussian density distributions.

The calculation is done by first-order perturbation theory, using the potential (9), the equations of motion in phase-amplitude form, and averaging the phase equation over many revolutions.

The ratios $\Delta Q_x/\Delta Q_{x0}$ and $\Delta Q_y/\Delta_{y0}$ are functions of the betatron amplitudes $\bar{x}/\sigma_x$ and $\bar{y}/\sigma_y$, and of the beam shape σ_y/σ_x. Tables of them are given in ref. 5.

The distribution functions can be obtained by a Monte Carlo technique, selecting initial amplitudes $\bar{x}$ and $\bar{y}$ according to a Rayleigh distribution which yields the desired Gaussian distribution of the charge density. This distribution is obtained from a uniform distribution of random numbers r in the interval [0, 1] by the transformation

$$\bar{z} = \sigma_z \sqrt{2}(-\ln(1 - r))^{\frac{1}{2}} \tag{40}$$

Examples of the tune shift distribution functions obtained are shown in Figs. 5 and 6. Typically, the tune spread is about half the linear tune shift. The consequences of this will be discussed below.

5. Computer Simulation of the Beam-Beam Effect

As an example, the computer simulation of the nonlinear lens experiment in the ISR will be described although it is not strictly speaking a simulation of the beam-beam effect. A test particle is created with initial conditions x_0, x_0', y_0, y_0' and is then followed for N turns, N being at least 10^4. A turn consists of two steps, the linear transformation around the machine, and the nonlinear kick. The transformation is described by a matrix

$$\begin{pmatrix} x \\ x' \\ y \\ y' \end{pmatrix}_{n+1} = \begin{pmatrix} \cos 2\pi Q_x & \sin 2\pi Q_x & 0 & 0 \\ -\sin 2\pi Q_x & \cos 2\pi Q_x & 0 & 0 \\ 0 & 0 & \cos 2\pi Q_y & \sin 2\pi Q_y \\ 0 & 0 & -\sin 2\pi Q_y & \cos 2\pi Q_y \end{pmatrix} \begin{pmatrix} x \\ x' \\ y \\ y' \end{pmatrix}_n \tag{41}$$

The kick is described by the following equations due to the particular shape of the nonlinear lens field

$$x'_{n+1} = x'_{n+1} - \frac{\pi\ \Delta Q_x}{d}\left(\ln\frac{(y-h)^2+(x+d)^2}{(y-h)^2+(x-d)^2} + \ln\frac{(y+h)^2+(x+d)^2}{(y+h)^2+(x-d)^2}\right)$$

$$y'_{n+1} = y'_{n+1} + \frac{2\pi\ \Delta Q_y}{d}\left[\tan^{-1}\left(\frac{x+d}{y-h}\right) - \tan^{-1}\left(\frac{x-d}{y-h}\right) + \tan^{-1}\left(\frac{x+d}{y+h}\right) - \tan^{-1}\left(\frac{x-d}{y+h}\right)\right] \tag{42}$$

Here, Q_x, Q_y, ΔQ_x, ΔQ_y and d are also input data.

The units of the co-ordinates are chosen so that the current bars have $y = \pm h$, and 2d is their width in the same units, as shown in Fig. 7. Examples of particle trajectories are shown in Figs. 8 and 9, the former showing an "unstable" one, and the latter a "stable" one. The distinction between "stable" and "unstable" trajectories is made a) by testing for $y > h$ which means that the particle hits the current bar, and b) by local instability. Local instability occurs when the distance in phase space between two particles which are very close initially, $\Delta x = 10^{-12}$, say, grows exponentially.

A complete survey of the stability behaviour by computer simulation requires variations of the initial amplitudes $(x_0^2 + x_0'^2)^{\frac{1}{2}}$ and $(y_0^2 + y_0'^2)^{\frac{1}{2}}$, of the tunes Q_x and Q_y and of the strength of the kicks ΔQ_x and ΔQ_y. This can be rather laborious, and time consuming on the computer. Much effort has been devoted to finding density distributions which yield algebraic expressions for the field components. A two-dimensional example is [6]

$$\rho = \frac{n\ e}{\pi\ a\ b}\left[1 + \frac{x^2}{a^2} + \frac{y^2}{b^2}\right]^{-2} \tag{43}$$

The field components are, as is easily verified

$$E_x = \frac{n\ e\ x}{2\pi\ \varepsilon_0\ a\ b}\left(1 + \frac{x^2}{a^2} + \frac{y^2}{b^2}\right)^{-1} \tag{44}$$

$$E_y = \frac{n\ e\ y}{2\pi\ \varepsilon_0\ a\ b}\left(1 + \frac{x^2}{a^2} + \frac{y^2}{b^2}\right)^{-1} \tag{45}$$

Unless done very carefully, it is not advisable to obtain the beam-beam forces by interpolation from tables. Discontinuities in their derivatives may cause instabilities in the simulation.

Computer simulations have been performed by many people, including Courant [7,8], Rees [9], Renieri [10]. The beam-beam limits found are in the range of experimentally observed beam-beam limits in e^+-e^- storage rings [11] for forces with continuous derivatives. When the forces have discontinuous derivatives the limit may be an order of magnitude smaller [8].

Almost by definition, computer simulation cannot establish the stability of a dynamical system, only its instability. Apart from this fundamental limitation, a practical limitation arises which is related to the number of turns which can be investigated. In a thorough survey which covers a whole range of initial conditions, tunes etc., the number of revolutions is of the order of 10^6. In the ISR, this corresponds to about 3 s, while the lifetimes of the beam are many hours. With today's computers, it would seem impossible to bridge this gap of 3 to 4 orders of magnitude.

6. Observation of Beam-Beam Effects in the ISR

6.1 Beam-beam effect of two coasting beams

From (28), the tune shift is for 30 A stacks at 26 GeV/c, $\beta_y^* = 14$ m, h = 3 mm

$$\Delta Q_y = 1.2 \times 10^{-3}$$

At this tune shift which is below the standard limit for protons, 0.005, the only observable beam-beam phenomenon is an increase in the decay rate corresponding to the total p-p cross section. All other observations can be explained by single beam phenomena. In particular, the observed growth of the beam height is compatible with intra-beam scattering [12].

6.2 Overlap knock-out resonances

Vertical beam growth and loss of protons from the top part of stacks have been observed while stacking with tunes close to an integer [13]. In this case the betatron frequencies F_β of the coasting beam begin to overlap the nearest frequencies F_s present in the longitudinal spectrum of the bunched beam at frequencies above 70 MHz. This suggests that the observed beam growth is due to the presence of transversely dangerous frequencies in the longitudinal spectrum of the bunched beam. One such mechanism is the kicks which the coasting beam receives due to the collisions with the bunched beam when the beams are not perfectly aligned at the crossing points. The two frequencies are given by

$$F_\beta = (n \pm Q_c)F_c = (n' \pm q_c)F_c \tag{46}$$

$$F_s = 30s\left(1 + \eta \frac{\Delta p}{p}\right)F_c \tag{47}$$

Here, n, n' and s are integers. Q_c is the tune, $q_c = 9 - Q_c$, and F_c the revolution frequency of the coasting beam. The factor 30 is the harmonic number of the ISR. The fact that 10 buckets are empty is neglected. $\Delta p/p$ is the momentum difference between bunched and coasting beam, and $\eta = \gamma_t^{-2} - \gamma^{-2}$, where γ_t is the transition energy. The bunch frequency spectrum extends to about s = 5. The frequencies (46) and (47) become equal when n' = 30s and

$$q_c = 30s\ \eta \frac{\Delta p}{p} \tag{48}$$

This relation between the tune q_c and $\Delta p/p$ is shown in Fig. 10.

Another way of describing this phenomenon consists in following a proton of the coasting beam and observing when it interacts with a bunch and when it crosses the interaction region in the gap between bunches. This behaviour is periodic with a period corresponding to many revolutions [14]. This fact permits one to obtain resonance widths, amplitude growths during crossing etc. by using the standard resonance calculation.

Experiments have demonstrated that the beam losses and growth observed during stacking are due to overlap knock-out resonances [13,14]. The resonance condition (48), the dependence on the beam separation and on the bunch frequency spectrum have all been verified. In addition to the beam-beam overlap knock-out resonances there is the corresponding phenomenon due to the bunched beam acting on the coasting beam in the same ring. Also, overlap knock-out resonances of higher order than first exist and have been measured.

An example of experimental results on overlap knock-out resonances is shown in Fig. 10a [14]. It shows the circulating current of an aperture-limited beam in Ring 1 as a function of the position of the bunched beam in Ring 2. The bunch moves from the right to the left, and beam losses are observed when it crosses dipole and quadrupole resonances.

6.3 The effect of a strong beam on a low-energy beam

One way of increasing the tune shift ΔQ_y given by (28) is to lower the energy γ_1 of the test beam while keeping the other parameters constant. This experiment has been carried out by K. Hübner [15].

A beam of 11.5 A was stored in one ring of the ISR, and afterwards, single pulses were injected into the other ring of the ISR at 2 GeV/c. The aperture for the weak beam was limited by vertical and horizontal scrapers. The lifetime of the weak beam was measured as a function of the current in the strong beam, and of the tunes Q_x and Q_y. The results obtained are shown in Table I.

Table I - Lifetime of the weak beams for different beam-beam tune shifts per intersection

ΔQ	I_s[A]	τ_1[min]	τ_2[min]	pulse No.
- 0.0043	11.5	21	30	7
- 0.0043	11.5	29	30	8
- 0.0017	4.5	34	29	9
- 0.0017	4.5	32	24	10
- 0.0	0	26	26	11

The lifetime τ_1 applies to a current of 5 mA in the weak beam. The lifetime τ_2 was measured 3 min after the aperture limits had been set. The most striking result is how short the lifetimes of the weak beam are: a fraction of an hour instead of many hours at higher energies. Within the errors of the measurement, no lifetime variation can be detected with the tune shift due to the presence of the strong beam. The conclusion of the experiment is that at a tune shift $\Delta Q_y \approx 0.0043$ there is no beam-beam effect which reduces the lifetime of an aperture-limited test beam to less than 20 or 30 minutes.

The short lifetimes observed can be explained by intra-beam scattering [12]. This is obvious from the observation that the lifetime of the weak beam depends on its own current as is shown in Table II.

Table II - Lifetime of an aperture limited 2 GeV/c beam as function of its current

I_w[mA]	6	5	4	3	2	1.5
τ[min]	14	20	23	29	35	39

Although this experiment did not provide the information on the beam-beam limit for protons which had been hoped for, it demonstrated the importance of intra-

beam scattering which is the dominant phenomenon determining the luminosity lifetime in the ISR.

6.4 Nonlinear lens experiment

Since it is not possible to increase the current in the ISR beyond certain limits, the beam-beam effect has been simulated by "colliding" a test beam with several hundred ampères circulating in a current bar over a distance of 0.867 m. The tune shifts achieved were $\Delta Q_y < 0.1$, i.e. well beyond the beam-beam limit for electrons.

In order to excite as many nonlinear field components as possible within the symmetry of the arrangement, the nonlinear lens (NLL) consists of two identical current bars which are parallel to the beam, one running above it and the other one below, as shown in Fig. 11. In order to concentrate as much field as possible in the vicinity of the beam, the current-carrying copper bar is surrounded by a U-shaped piece of high-permeability alloy. The field generated approximates that of the infinitely thin current sheet shown in Fig. 7. The field components are implicitly given in (42).

The effect of the NLL was determined by measuring the lifetime of the beam for which the aperture was limited by the NLL itself, as a function of the NLL current and the tunes in the machine. The results are shown in Table III and in Fig. 12. Table III shows how the decay rate varies with the machine tunes at a given excitation of the NLL. There are large variations even for tune changes much smaller than the tune spread present in the beam due to the NLL. Fig. 12 shows the variation of the decay rate with the excitation of the NLL. The decay rate varies over 3 orders of magnitude when the linear tune shift ΔQ_y is changed from 0 to 0.1. The saturation of the decay rate occurs close to the stochasticity limit found by computer simulation as described in section 5. There are too few experimental data available for small tune shifts ΔQ_y to make definite statements about a possible threshold for the beam loss.

Table III - Beam decay rates in units of 10^{-5} s^{-1} with the NLL excited to $\Delta Q_y = -0.054$.

ΔQ_y	ΔQ_y		
	- 0.0025	0	+ 0.0025
0.0025	7.8 ± 0.8	12.8 ± 2.1	17.3 ± 2.6
0	1.5 ± 0.1	7.0 ± 0.5, 3.0 ± 0.2	1.7 ± 0.2
- 0.0025	0.6 ± 0.03	0.5 ± 0.07	0.6 ± 0.04

6.5 Beam-beam effect in a high-β insertion

It is obvious from (28) that the beam-beam tune shift can be raised by increasing β_y^* at the crossing point. This experiment has been done by Zotter [17]. A high current is stored in one ring of the ISR, while the other ring is modified to include a crossing at a high value of β_y^*. This is done by exciting the quadrupoles of the low-β insertion [18] in a different manner. In order to enhance the effect of β_y^*, the energy in the second ring is 11 GeV. With $\beta_y^* = 200$ m and a circulating current of 15 A with an effective height of 5 mm, a tune shift $\Delta Q_y = 0.017$ can be reached according to (39).

In order to detect an increase in the betatron amplitude of the weak beam its size is restricted by scrapers while its lifetime is measured. It turns out that the setting up of the experiment is rather time consuming because it is so far away from normal operating conditions in the ISR. So far, very few data have been taken, Fig. 13 shows the variation of the beam lifetime with the current of the strong beam obtained.

So far the experimental results are very confusing. More experiments are foreseen in the future.

Conclusions

It was first pointed out by Chirikov [19] that there might be a slow mechanism for amplitude growth which he called Arnold diffusion. Because of its slowness the phenomenon cannot be observed in electron machines since there all growth mechanisms with growth rates less than the synchrotron radiation damping rate are masked. On the basis of Chirikov's work, an estimate of a limiting beam-beam tune shift $\Delta Q = 0.005$ was obtained [20]. This has since become the conventional limit to which several proton storage rings have been designed. There has not been any recent theoretical work to confirm or to invalidate this limit. The experimental work has been inconclusive.

REFERENCES

1) B. Houssais; private communication, Univ. de Rennes (1967).

2) E. Keil, C. Pellegrini, A.M. Sessler; NIM 18, 185 (1974).

3) B.W. Montague; CERN Report ISR-GS/75-36 (1975).

4) A. Jejcic and J. le Duff; VIIIth Int. Conf. on High Energy Accelerators, CERN 1971, 354.

5) E. Keil; CERN Report, ISR-TH/72-7 (1972).

6) L.J. Laslett; PEP-91 (1974).

7) E.D. Courant; IEEE Trans. Nucl. Sci. NS-12, 650 (1965).

8) E.D. Courant; 1975 Isabelle Summer Study, BNL 20550 Vol. I.

9) J.R. Rees; Int. Symp. Electron and Positron Storage Rings, Saclay 1966, VII-7.

10) A. Renieri; 1973 PEP Summer Study, PEP Note 72.

11) F. Amman; IEEE Trans. Nucl. Sci. NS-20, 858 (1973).

12) A. Piwinski; IXth Int. Conf. on High Energy Accelerators, Stanford 1974, 405.

13) H.G. Hereward and S. Myers; private communication.

14) J.P. Gourber and C. Wyss; private communication.

15) K. Hübner; IXth Int. Conf. on High Energy Accelerators, Stanford 1974, 63.

16) E. Keil and G. Leroy; IEEE Trans. Nucl. Sci. NS-22, 1370 (1975).

17) B. Zotter; private communication.

18) J.P. Gourber, E. Keil and S. Pichler; IEEE Trans. Nucl. Sci. NS-22, 1419 (1975).

19) B.V. Chirikov; Institute of Nuclear Physics, Novosibirsk, Preprint 267, section 4.3

20) E. Keil; VIIIth Int. Conf. on High Energy Accelerators, CERN 1971, 372.

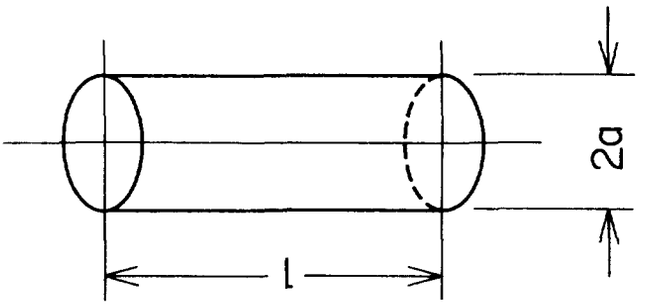

Fig. 1 Cylindrical bunch

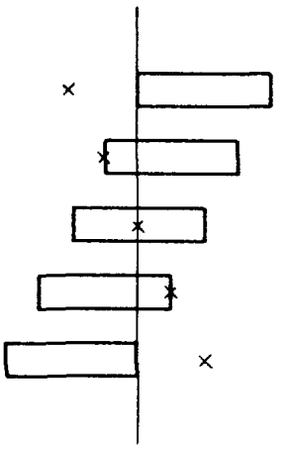

Fig. 2 Collision between test particle and bunch

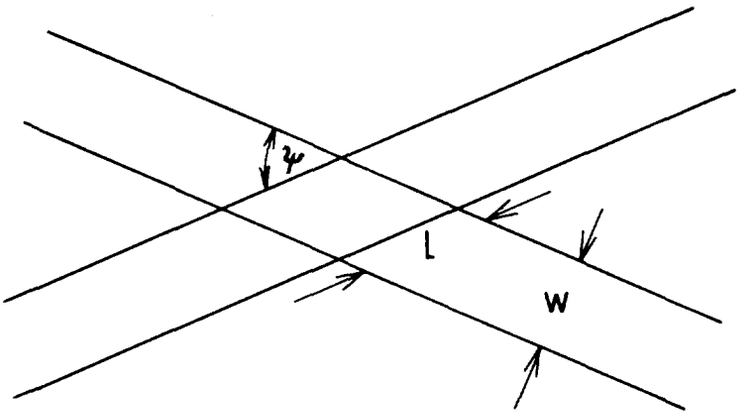

Fig. 3 Large angle crossing

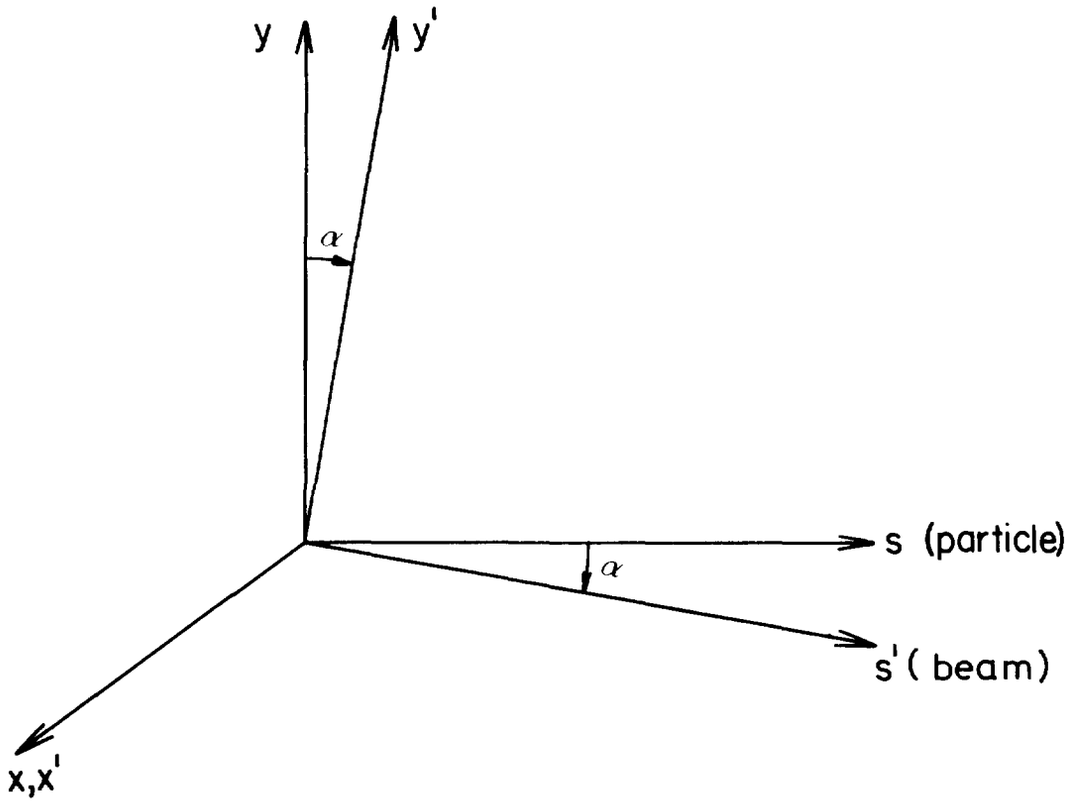

Fig. 4 Co-ordinate system for small crossing angle

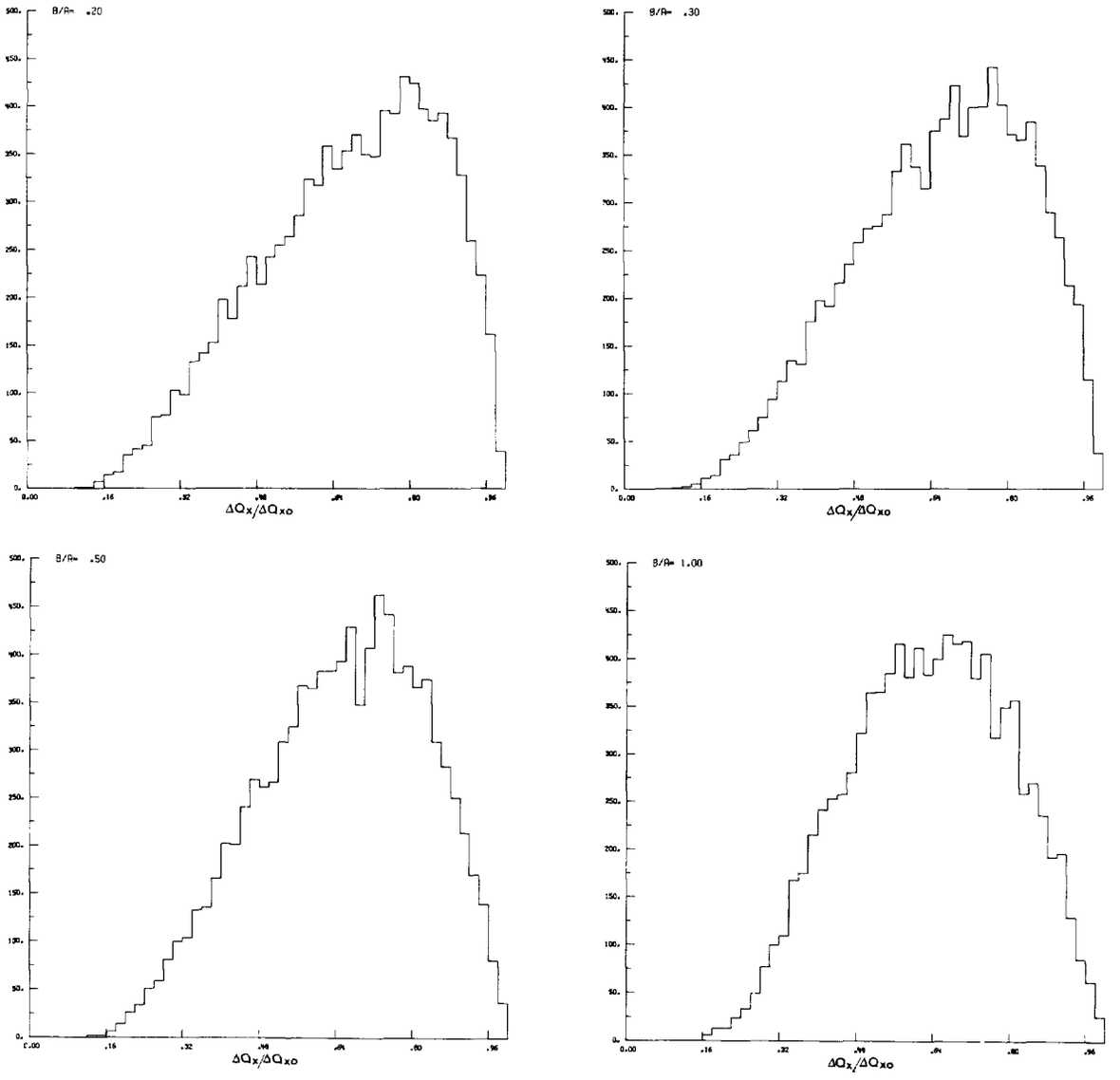

Fig. 5 Tune shift distribution function

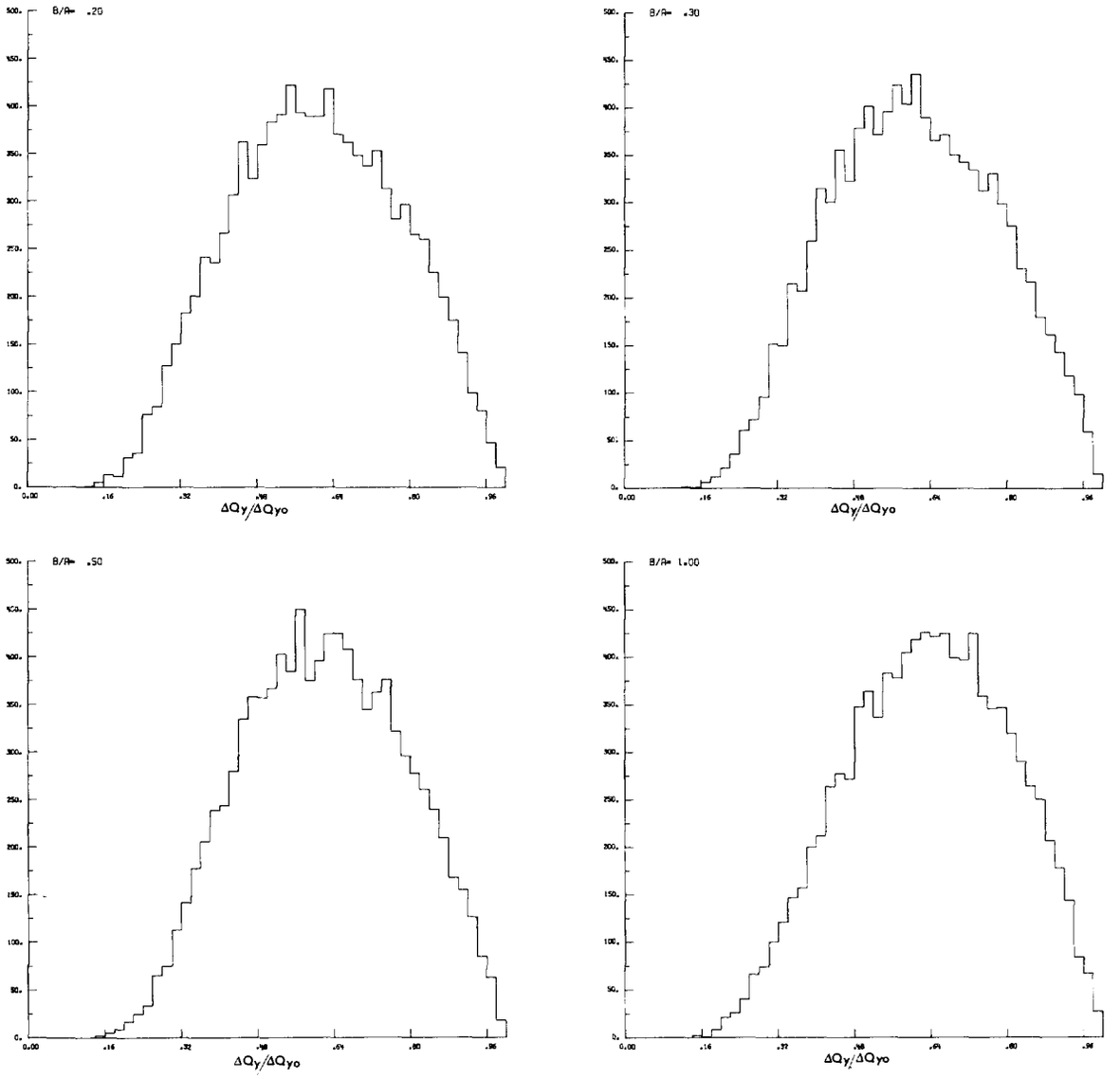

Fig. 6 Tune shift distribution function

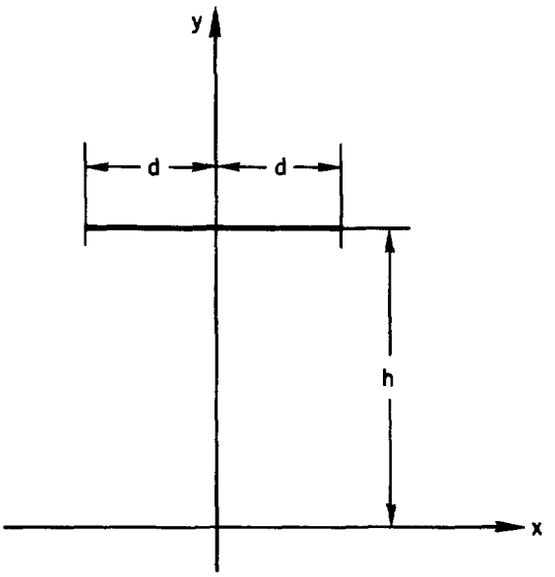

Fig. 7 Scheme of nonlinear lens

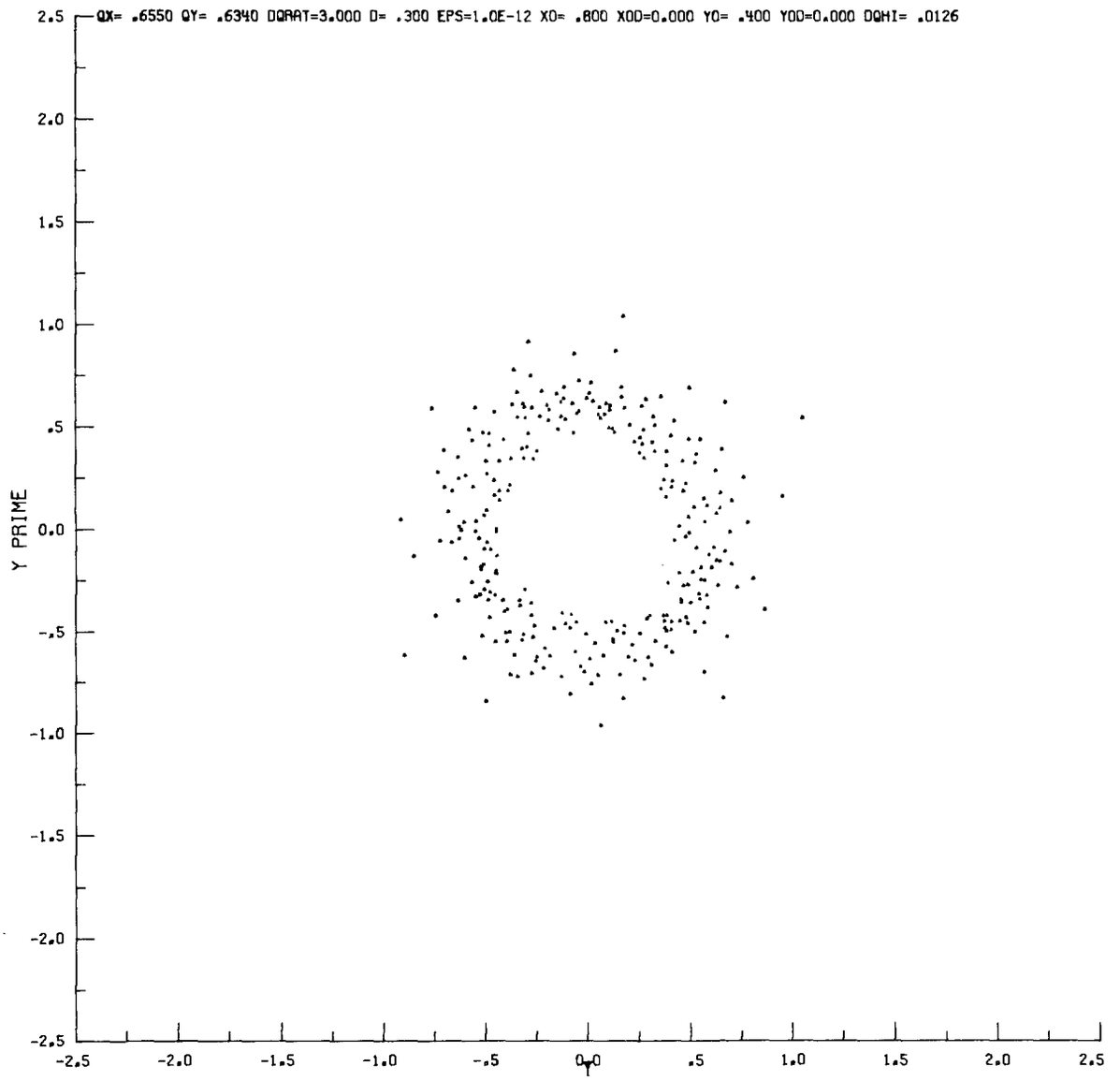

Fig. 8 Unstable phase space diagram

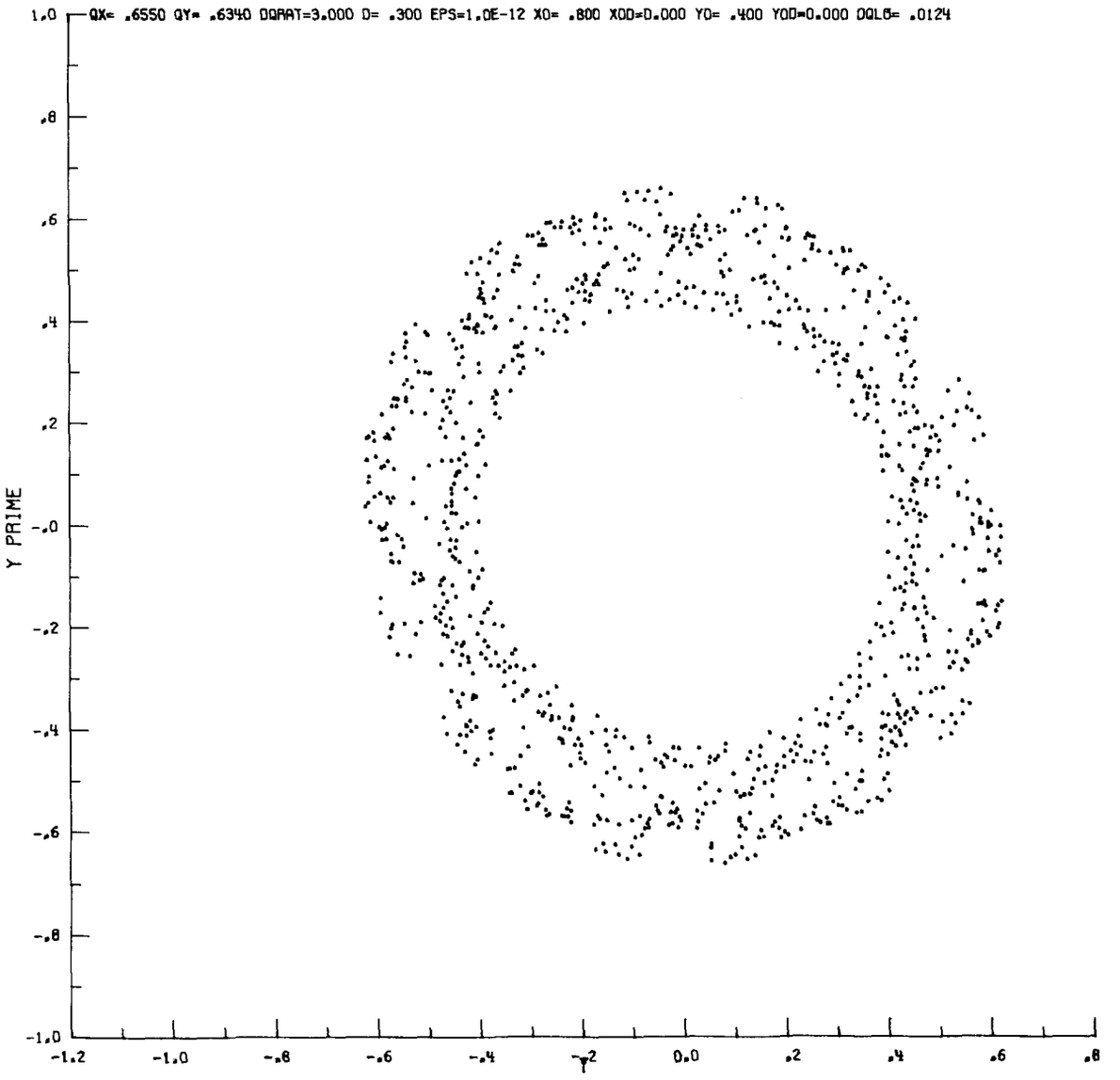

Fig. 9 Stable phase space diagram

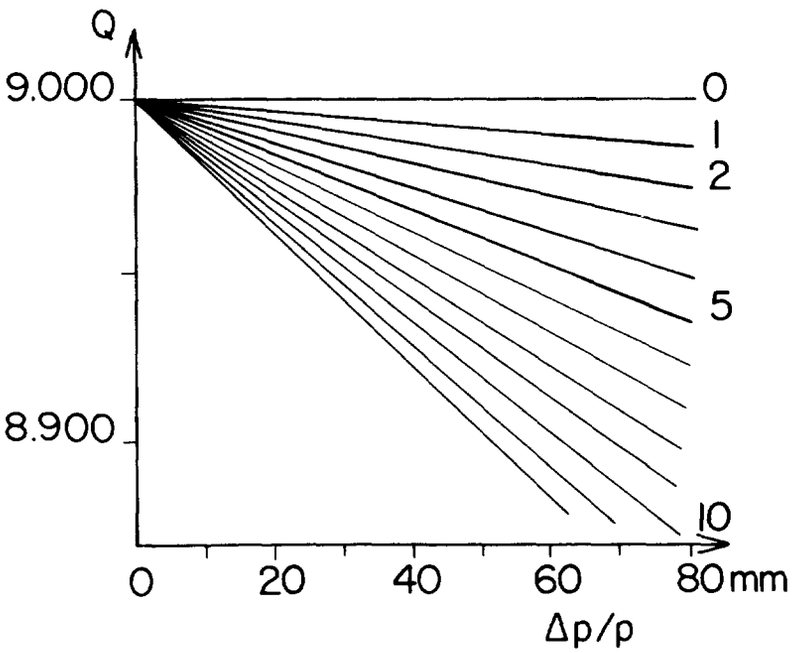

Fig. 10 Frequencies for overlap knock-out

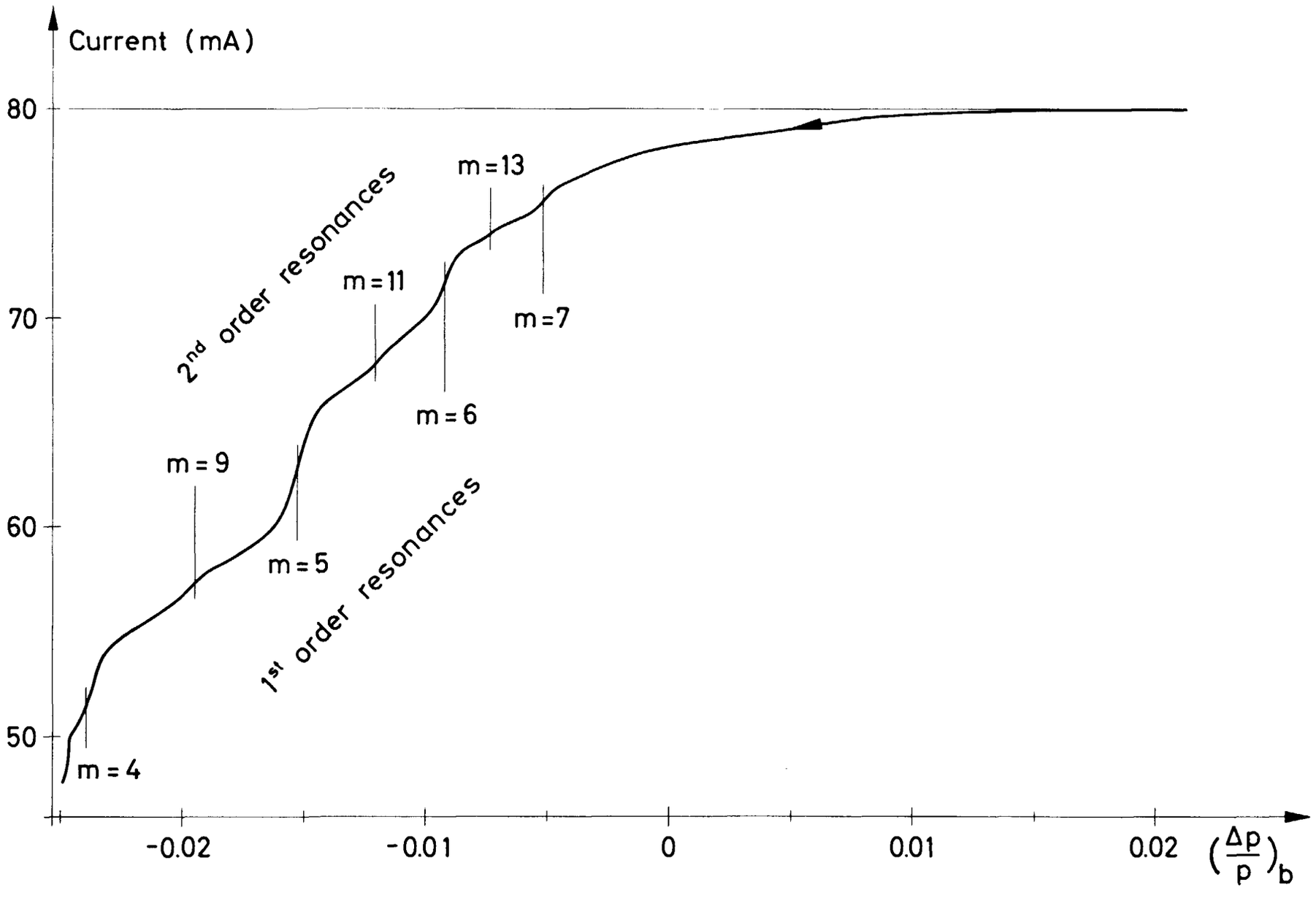

Fig. 10a 1st and 2nd order overlap knock-out resonances

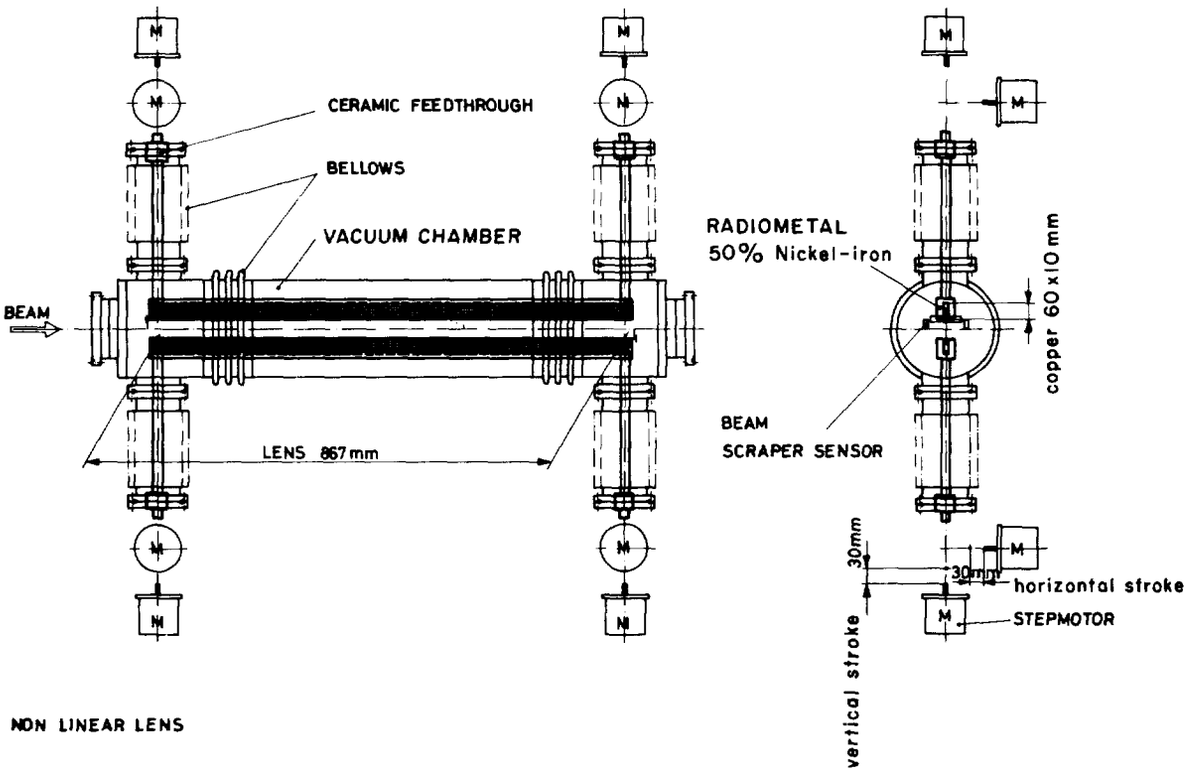

Fig. 11 View of nonlinear lens

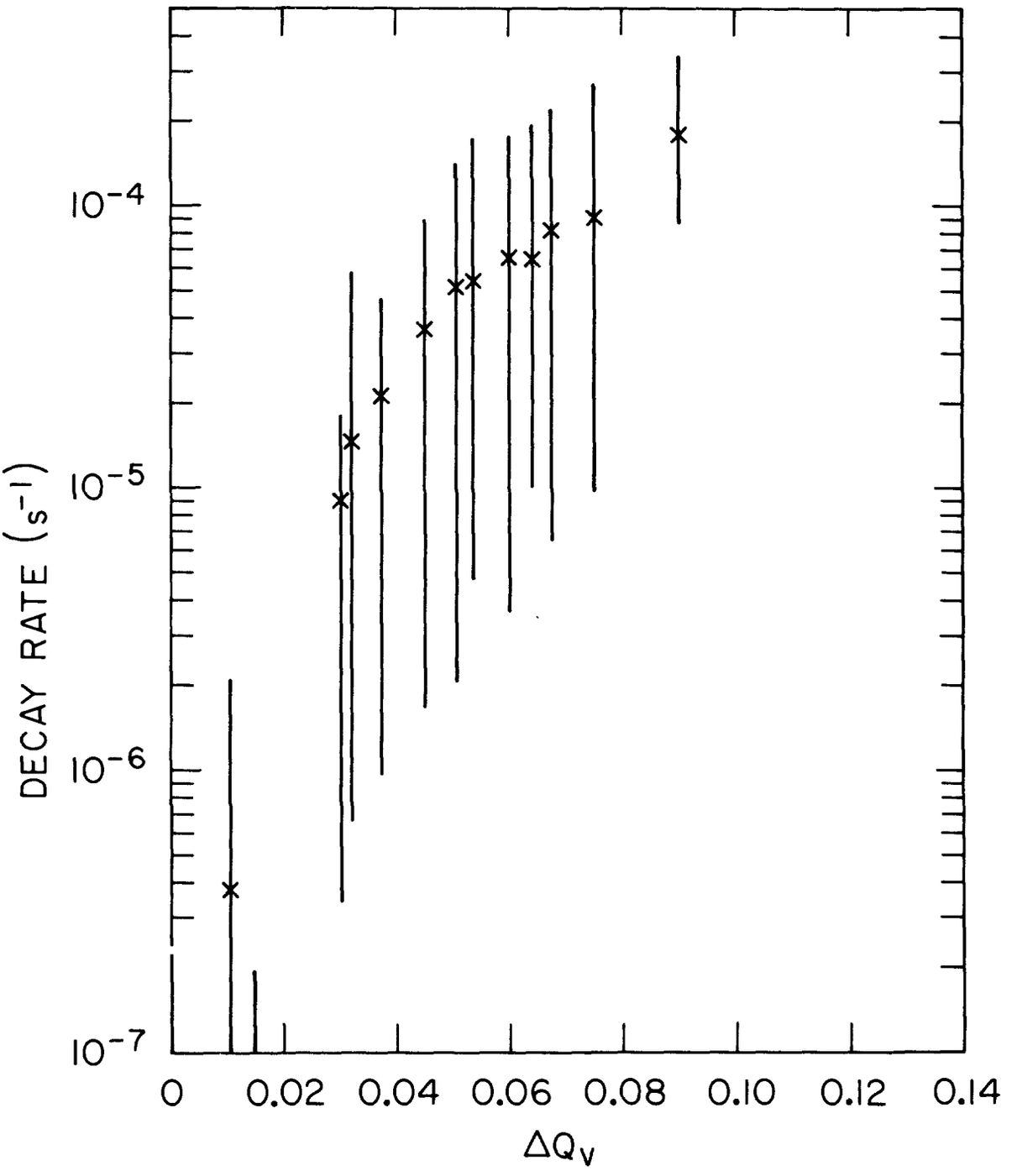

Fig. 12 Decay rate vs. nonlinear lens current

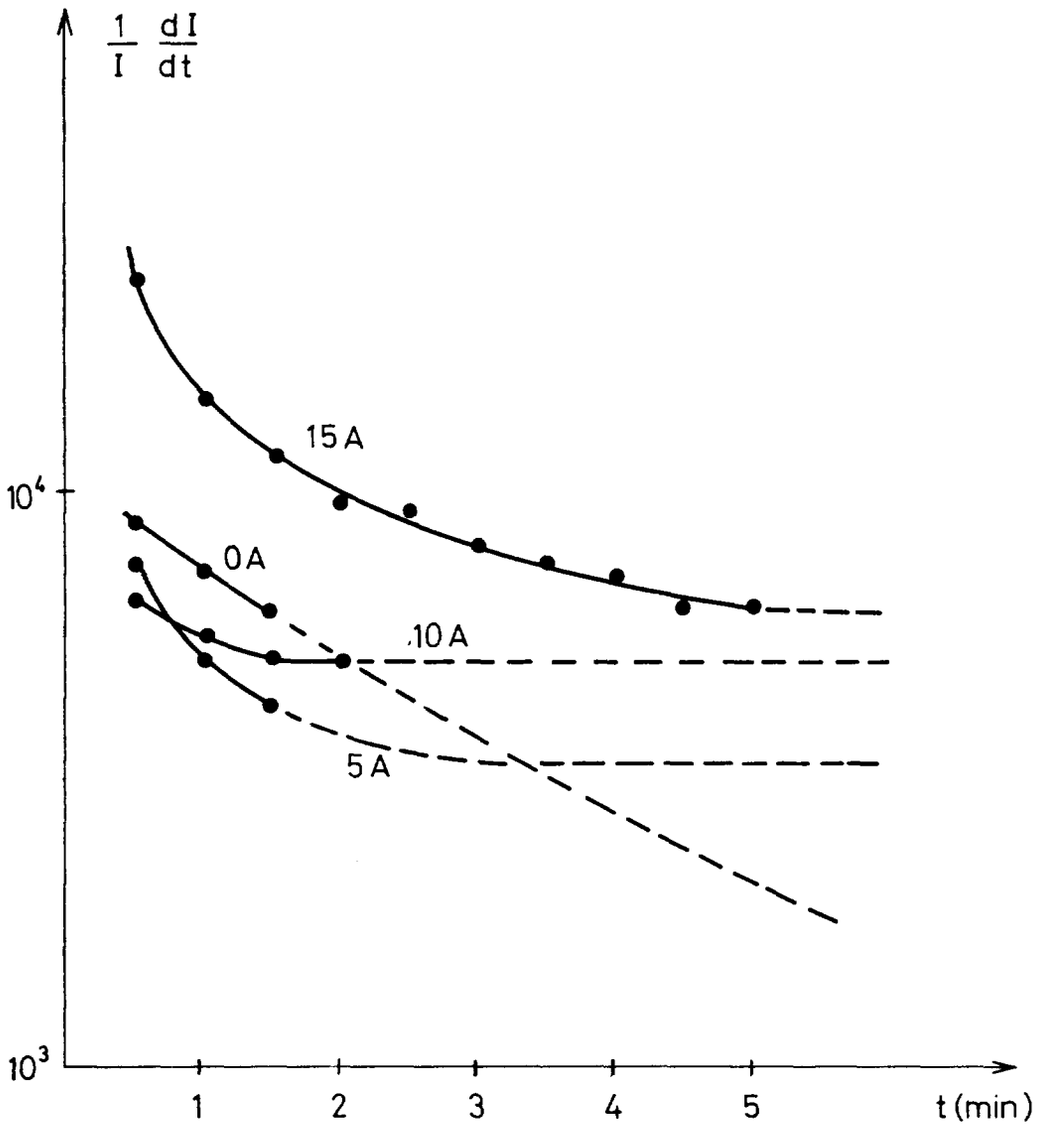

Fig. 13 Decay rate vs. stacked current (high-β)